

Influence of Tip Clearance and Inlet Flow Distortion on Ducted Fan Performance in VTOL UAVs

Ali Akturk

Graduate Research Assistant

Vertical Lift Research Center of Excellence (VLRCOE)

The Pennsylvania State University

University Park, PA

aua162@psu.edu

Cengiz Camci

Professor of Aerospace Engineering

Vertical Lift Research Center of Excellence (VLRCOE)

The Pennsylvania State University

University Park, PA

cxc11@psu.edu

ABSTRACT

Ducted fan vertical take-off and landing (VTOL) uninhabited aerial vehicles (UAV) are popular because they offer higher disk loading compared to open rotors and improve propulsive performance. Although ducted fans provide high performance in many VTOL applications, there are still unresolved problems associated with them especially in the forward flight mode. The main problems in these applications are distortion of inlet flow due to forward flight and tip leakage related problems in hover and forward flight modes. The present experimental study mainly uses total pressure measurements downstream of a ducted fan rotor to investigate the performance drop in hover and forward flight condition related with these problems. Tip leakage flow related total pressure losses are dominant in hover condition. Losses are dramatically increased in forward flight due to inlet lip separation and inlet flow distortion. For a better comparison of the tip clearance effects in forward flight, a new parameter named as "Forward flight penalty" is defined. In addition to comprehensive aerodynamic loss measurements downstream of the rotor, the paper also discusses the results from the early stage of a computational study aiming to calculate the 3D turbulent viscous flow in and around the ducted fan.

NOTATION

P_a	= Atmospheric pressure
P_T	= Total pressure (Pa)
Cp_{Total}	= Total pressure coefficient
Ω	= Rotational speed (radian/sec)
r	= Radial distance measured from origin
ρ	= Density
R	= Universal gas constant (joule/kg.K)
T_a	= Atmospheric temperature (Kelvin)
V_{ref}	= Reference velocity (m/s)
R_{Tip}	= Tip radius (m)
D_R	= Fan rotor diameter (m)
D	= Shroud diameter (m)
FFP	= Forward flight penalty

INTRODUCTION

Military uninhabited air vehicle developers has a great interest in ducted fan vertical take off and landing (VTOL) unmanned aerial vehicles (UAVs). These UAVs can hover in one location, as well as take off and land vertically. In addition to conventional military tasks, they can continuously transmit surveillance data and act as a relay station. Although ducted fans may provide high performance in many VTOL applications, there are still unresolved problems associated with them especially in the forward

flight mode. Although early full scale ducted fan based air vehicles such as Bell X-22A and DOAK VZ-4 provided a significant amount of information and operational data, the ducted fan performance issues related to inlet lip separation and tip clearance problems still contribute to the performance issues in present day systems.

Experimental investigation has been one of the major approaches to study the flow characteristics of ducted fans. Abrego and Bulaga [1] performed wind tunnel tests to determine the performance characteristics of ducted fans for axial and forward flight conditions. Their study resulted in the clarification of the important effect of exit vane flap deflection and flap chord length in providing side force. Fleming, Jones and Lusardi et al. [3] conducted wind tunnel experiments and computational studies around a 12-in diameter ducted fan. They have concentrated on the performance of ducted fan VTOL vehicles in crosswind.

Graf, Fleming and Wings [4] improved ducted fan forward flight performance using a newly designed leading edge geometry which has been determined to be the significant factor in offsetting the effects of the adverse aerodynamic characteristics.

Akturk, Shavalikul and Camci [5] experimentally investigated complicated flow field around the ducted fan in hover and forward flight conditions. Flow features such as inlet lip separation, distortion of inlet flow features before

and after the axial fan rotor, influence of rotor tip speed, influence of forward flight velocity and the interaction of the cross wind with fan exit jet are investigated through planar particle image velocimetry (PIV) experiments. An actuator disk based three dimensional viscous flow computation of the specific ducted fan system is also presented.

Mort and Yaggy [6, 7] performed hover and forward flight tests on 4-foot diameter wing tip mounted ducted fan that is used on Doak VZ-4-DA. Performance characteristics for ducted fan were reported.

Mort and Gamse [8] investigated aerodynamic characteristics of a 7- foot diameter ducted propeller which was used on the Bell Aerosystems X-22A airplane. They reported aerodynamic characteristics for variations of power, free-stream velocity, blade angle, and duct angle of attack. Stall of both the upstream and downstream duct lips of this seven foot diameter ducted fan was examined in function of angle of attack. It was found that the onset of separation on the upstream lip will be encountered; however, complete separation on this lip will be encountered only during conditions of low power and high duct angle of attack.

Martin and Tung tested a ducted fan VTOL UAV with a 10-in diameter fan rotor [2]. They measured aerodynamic loads acting on the vehicle for different angle of attacks in hover and different crosswind velocities. They also included hot wire velocity surveys at inner and outer surface of the duct and across the downstream wake. The effect of tip gap on the thrust force produced was emphasized. They underlined the importance of tip vortex and duct boundary layer interaction. In addition, their study showed the effect of leading edge radius of duct on the stall performance and stability of the vehicle.

The current experimental study uses total pressure measurements at the exit of the fan rotor to investigate effect of tip leakage flow in hover and forward flight condition. Special attention is paid in obtaining forward flight related experimental data near the tip region of the rotor where complex tip leakage flow and low momentum re-circulatory flow from the inlet lip separation area interacts. By the high resolution total pressure measurements, effect of duct flow on fan rotor exit performance was investigated in forward flight. Measurements were obtained at various circumferential positions so that the inlet flow distortion effect on rotor performance was investigated. The main purpose of this study is to show how tip leakage flow behaves in the presence of forward flight velocity. The second purpose is to understand how rotor exit flow field is affected from the inlet flow distortions caused by forward flight velocity.

EXPERIMENTAL SETUP

Penn State Mid-sized Wind Tunnel

The tests for this study were performed in Penn State mid-sized wind tunnel. This wind tunnel is a closed circuit,

single return tunnel type. Figure 1 shows a schematic of the wind tunnel layout. A contraction section with an area ratio of 9.9:1, accelerates the flow to obtain a higher flow velocity in the test section. The maximum tunnel flow speed is 145 ft per second. The test section has a typical turbulence intensity of 0.6 % .

A test section has a rectangular cross section with two feet wide, three feet tall and 20 feet in length dimensions.

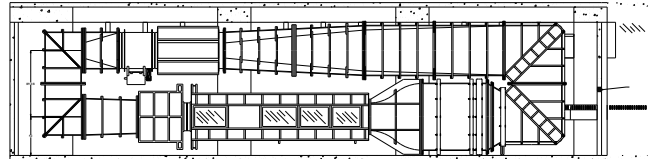


Figure 1. Mid-sized wind tunnel at Penn State University.

Ducted Fan Model

The current study deals with ducted fan experiments in a wind tunnel environment simulating the hover and forward flight of a VTOL UAV system as shown in Figure 2. The current research program maintains a disk loading range from 5 to 35 lbf/ft² in a corresponding rotor speed range from 5000 rpm to 20,000 rpm.

The brushless DC electric motor driving the five-bladed ducted fan rotor is speed controlled by an Castle creation HV-110 electronic speed control (ESC) system. The high efficiency Neu 1521/1.5Y electric motor driving the fan can deliver 2.14 HP power (1.5 KW).



Figure 2. Wind tunnel model simulating VTOL UAV at forward flight.

Figure 3 shows the five bladed ducted fan rotor that is used in the present experimental study. The main geometric parameters of the rotor system are presented in Table 1. This ducted fan unit manufactured from carbon composite material

is designed for small scale uninhabited aircraft. Six outlet guide vanes remove some of the swirl at the exit of the rotor. A tail cone is used to cover the motor surface and hide the electrical wiring for the wind tunnel model.

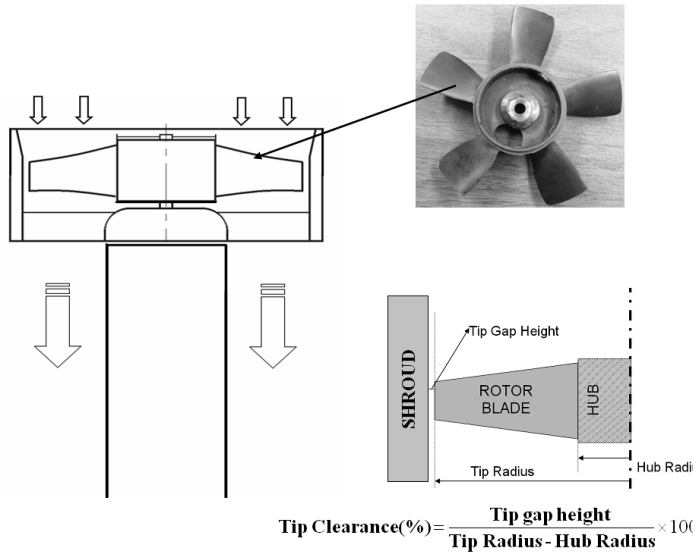


Figure 3. Ducted fan, five-bladed fan rotor and tip clearance definition.

An optical once-per-revolution device located near the hub of the rotor exit is used for measurement of rotational speed of the fan rotor.

Tip clearance was calculated based on blade height which is the length of the blade from hub to tip. Calculation of tip clearance is shown in figure 3. Tip clearance value of the ducted fan was adjusted by using different shrouds each manufactured for a specific tip gap size. Shroud of the ducted fan used in experiments were made of transparent plexiglass material. Table 1 shows used tip clearances for the experiments and corresponding inner diameters of shrouds.

Table 1. Geometrical parameters of the ducted fan

Characteristic	English	Metric
<i>Rotor hub diameter</i>	2.02 inches	52 mm
<i>Rotor tip diameter</i>	4.69 inches	120 mm
<i>Rotor Blade Span</i>	1.34 inches	34 mm
<i>Max. blade thickness @ tip</i>	0.06 inches	1.5 mm
<i>Shroud inner diameter for %5.8 tip clearance</i>	4.84 inches	122.9 mm
<i>Shroud inner diameter for %3.6 tip clearance</i>	4.78 inches	121.4 mm

The ducted fan system was supported by a steel support shaft connected to the center of the tailcone. The steel support shaft was held in place by two linear bearings to minimize friction while effectively isolating only the thrust associated with the ducted fan.

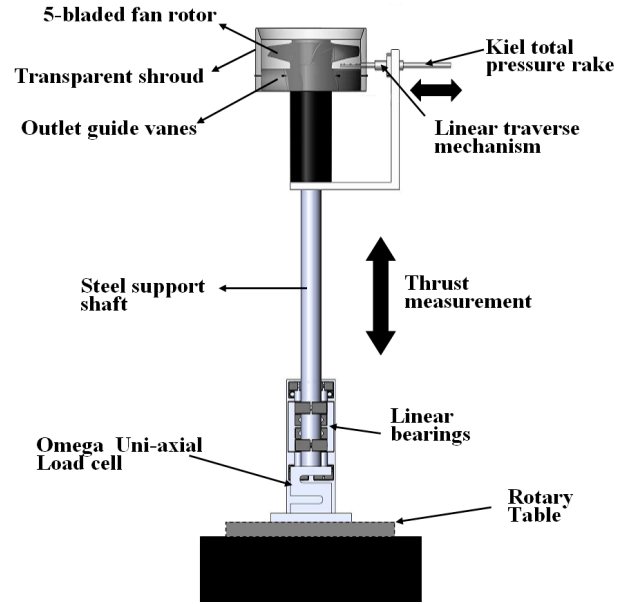


Figure 4. Sketch of ducted fan test system.

Instrumentation

The ducted fan test system was equipped with a Kiel total pressure rake, which was mounted on linear traverse system, and a uni-axial load cell, which was located under the steel support shaft. Figure 4 shows a sketch of the ducted fan test system.

The test system was positioned on top of a precision rotary table for total pressure measurements at different circumferential positions.

Thrust Measurements

Thrust of the ducted fan was measured by 25 lbf (11.34 kgf) Omega LCCA-25 uni-axial load cell for hover condition. The load cell was connected to the steel support and mounted on a plate which is attached to the rotary table. This load cell was connected to an Omega model DP25B-S strain gage signal conditioner including a panel meter. The meter provided a 10 V excitation voltage, and conditioned the returning signal. The output of the load cell was previously calibrated by applying known static loads. Tabulated accuracy of the load cell is 0.037% of the full scale load.

Total Pressure Measurements

Fan rotor exit total pressure measurements were performed by using a "United Sensors Type A" Kiel total pressure rake system as shown in Figure 5. The Kiel total

pressure rake having five 2 mm total heads was traversed in radial direction using a precision linear traverse mechanism.

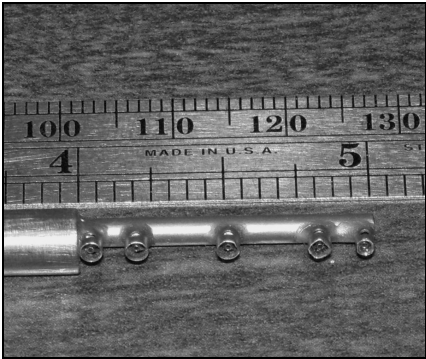


Figure 5. United Sensors Kiel total pressure rake.

Total pressure rake was typically located 10 mm downstream of the fan rotor exit plane at %50 of blade span (mid-span). The Kiel probe was aligned with absolute rotor exit velocity at mid span position. Figure 6 shows the velocity triangle of the rotor blade section and position of the Kiel probe.

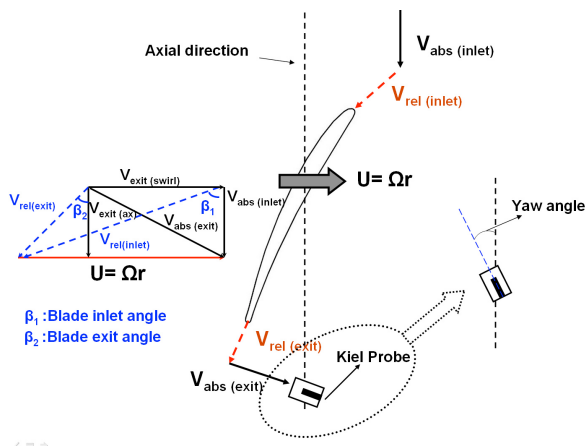


Figure 6. Rotor exit velocity triangle and orientation of Kiel probe.

United Sensors type A Kiel probe is relatively insensitive to incoming angle of the flow (yaw angle). The range of insensitivity to misalignment for this probe is $\pm 52^\circ$ to see a more than 1 % deviation from the inlet dynamic head [9]

Five Kiel total pressure heads in the rake system were connected to a 40-port Scanivalve system with 1/8" tubing that was 5ft long. The Scanivalve was used to take all the pressure measurements. The Scanivalve was connected to a Validyne CD-15 pressure transducer that was referenced to atmospheric pressure.

The calibration of the pressure transducer required applying a known pressure to the transducer and recording the associated voltage. The relationship between the pressure and voltage was linear. The Validyne pressure transducer

was connected to a Fluke 45 Dual Multimeter. The measured settling time of the system used in this project was 40 seconds, so the Kiel probe pneumatic output reached an equilibrium and mass averaged total pressure reading recorded.

EXPERIMENTAL RESULTS AND DISCUSSION

In the current study, the aerodynamic performance of the ducted fan used for VTOL UAVs was quantified by measuring radial distribution of fan rotor exit total pressure for both hover and forward flight. The effect of tip leakage flow on fan rotor performance was also investigated. Thrust measurements were performed in hover condition for various rotational speeds.

Total pressure results were expressed in non-dimensional form as total pressure coefficient throughout the paper.

$$Cp_{Total} = \frac{P_t - P_a}{\frac{1}{2} \rho V_{ref}^2} \quad \text{where } \rho = \frac{P_a}{RT_a} \quad (1)$$

The reference velocity used in equation 1 was calculated from the fan rotor tip speed.

$$V_{ref} = \Omega \cdot R_{Tip} \quad (2)$$

All the radial coordinates are given in non-dimensional form (r / R_{Tip}) throughout the paper.

Hover Condition Results

Thrust measurements were obtained at hover condition for various rotor speeds. Thrust measurements were normalized as disk loading which is thrust force per unit rotor disk area. Disk loading parameter is a significant indicator of how a rotor disk is fluid mechanically loaded as a result of a complex energy addition process to air in a fan rotor passage. The flow quality in a fan rotor passage is directly controlled by the adverse pressure gradients and highly re-circulatory/turbulent flow conditions.

Three different configurations are compared in figure 7 including a fan rotor “without shroud” and two shrouds having specific tip clearances (5.8 and 3.6 %). Figure 7 shows that adding a shroud to the fan system increased the thrust leading to improved rotor disk loading. At higher rotational speeds, adding shroud improved rotor disk loading as much as %24. Two different shrouds with different tip clearances are also compared in figure 7. Decreasing the tip gap height increased the thrust and disk loading. Figure 8 shows radial distribution of total pressure coefficient for two tip clearances at 12000 rpm in hover condition. Increasing the tip gap height increased leakage flow at the tip and reduced performance of the fan rotor. The existence of a significant tip leakage vortex in the rotating passage

generated complex 3D flow patterns, aerodynamic losses and unsteady flow patterns. Decreasing the tip clearance resulted in approximately %20 increase in the measured total pressure at the rotor exit at mid span location .

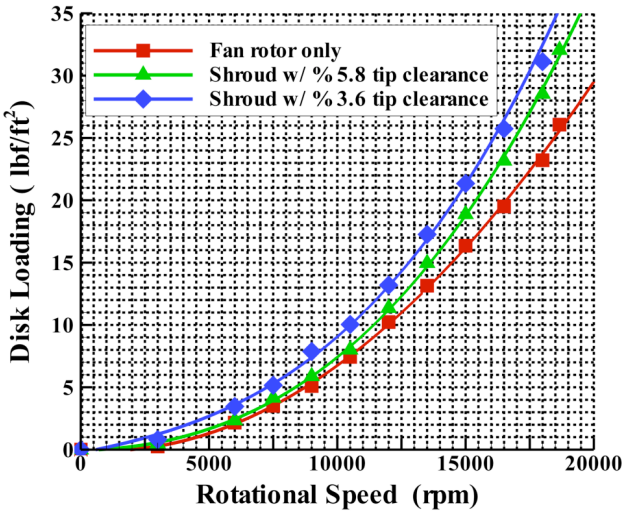


Figure 7. Disk loading versus rotational speed at hover condition for the current VTOL UAV wind tunnel model

Total pressure increment generated by the fan rotor was reduced near the tip region for both clearances. That reduction in total pressure was due to tip leakage flow originating at the rotor tip. For %5.8 tip clearance, total pressure started to drop at $r/R_{Tip} > 0.88$ visibly. However, for the reduced tip clearance of %3.6, it started to drop where

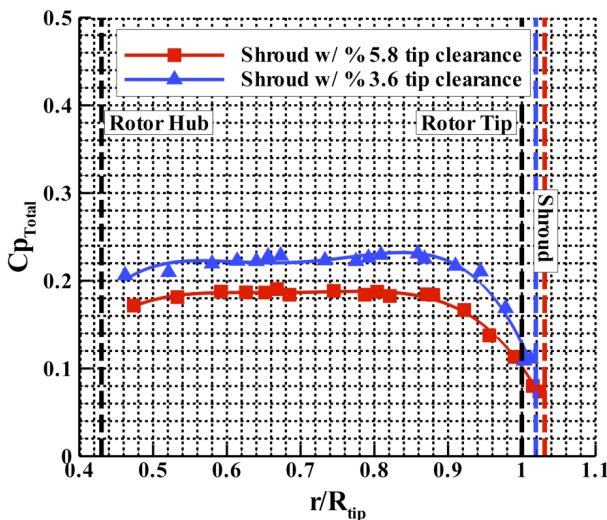


Figure 8. Radial distribution of total pressure coefficient at 12000 rpm hover condition

$r/R_{tip} > 0.92$. The smaller tip clearance provided a higher overall total pressure near the tip section of the blade. The

energy addition ability of the rotor to the flow near the tip section was hindered by the adverse effects of the tip leakage flow.

Forward Flight Results

Forward flight experiments were performed in Penn State mid-sized wind tunnel. As mentioned in the previous sections, ducted fan system was mounted on top of rotary table for circumferential movements. The test system was positioned inside the wind tunnel test section such that the interaction of ducted fan and boundary layer of the wind tunnel walls were effectively minimized. The test system was positioned so that the ducted fan was 3 rotor diameters (D_R) away from the top wall, 4.5 D_R away from the bottom wall and 2.8 D_R away from the side walls. For the measurements of upstream velocity of ducted fan, a hot-wire anemometer is positioned 4.5 D_R upstream of the duct. A sketch of experimental setup for wind tunnel measurements is shown in figure 9.

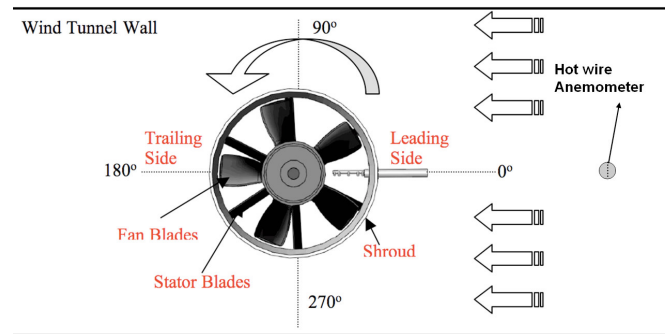


Figure 9. Wind tunnel experimental setup for forward flight condition.

The windward side of the ducted fan is named as the leading side and leeward side of it is named as the trailing side throughout the paper. For forward flight conditions, four different circumferential stations were considered. First circumferential position was 0° as shown in figure 9. Total pressure rake was aligned with the leading side of the ducted fan. Other circumferential locations were obtained by turning the test system 90° , 180° and 270° in counter-clockwise direction. In each circumferential direction, the radial distribution of total pressure was measured for 12000 rpm rotational speed and 10 m/s forward flight velocity.

Forward Flight Flow Visualization

Effects of forward flight on the flow field around the duct can be better understood by the help of a smoke flow visualization technique. This technique utilized a thin 0.12 mm diameter 30 cm long stainless steel wire. The wire was carefully coated with a glycerol layer before each experiment. The wire was heated to the glycerol evaporation temperature, producing visible smoke for up to three seconds in the lowest speed cases. A few strips of white LEDs and

strips of UV LEDs were used for visualization. The camera used for the visualization study was a three chip high resolution Sony DCR VX 2000 digital camera. For the best visualization, the camera viewing angle was kept perpendicular to both the wire and the direction of incidence of the light on the field of view.

Figure 10 shows a smoke flow visualization image obtained at 5m/s wind tunnel speed and 6000 rpm rotor speed. Introducing forward flight is clearly disturbing the inlet flow characteristics of the ducted fan system. Non uniformities can be seen in the side view images. Flow near the leading side is approaching to the duct lip with a significant momentum in the radial direction (fan) that is the same as the wind tunnel flow direction. Existence of the duct lip is a major obstacle in turning the almost horizontal inlet flow into the axial direction of the fan. A severe inlet flow distortion near the lip section of the fan unit is observed. The wind tunnel flow approaching the fan shroud as a blunt object stagnates over the external part of the shroud. This flow tries to reach the lip section of the shroud and turns around it to be part of the axial fan rotor energy addition process. Due to high adverse pressure gradient at the leading side duct lip, a separation flow region near the leading edge of the lip section (before the rotor entrance plane) occurs. This flow separation which is also known as inlet lip separation partially blocks inlet of the fan rotor at the leading side. The air breathing ability of the fan rotor is adversely affected from the lip flow separation occurring under forward flight conditions.

Forward Flight Total Pressure Results

Figure 11 shows total pressure distribution measured at the exit of the fan rotor for different circumferential stations at hover and forward flight condition. Measurements were obtained at 12000 rpm rotational speed and 10 m/s forward flight velocity with shroud that has a %5.8 tip clearance.

The highest level of measured loss due to forward flight occurred at the leading side. By the effect of inlet lip separation and distortions in the inlet flow, a considerable defect in measured total pressure was noticed for $r/R_{Tip} > 0.7$. Especially for $r/R_{Tip} > 0.9$, total pressure losses increased tremendously compared to that of the hover condition. The adverse effects of tip leakage flow on the fan rotor performance was worsened by forward flight conditions. Distortions at the inlet flow of the fan rotor and inlet lip separation reduced the energy addition capability of the tip section of the rotor blade and resulted in a performance loss spread over approximately % 80 of blade span. Losses were especially increased around the tip region, near the leading side. Since tip clearance was not changed between hover and forward flight conditions, losses generated near the casing due to transition to forward flight are directly related to inlet lip separation and losses because of distorted inlet flow. It was also noted that for $r/R_{Tip} < 0.55$, there was a significant amount of total pressure loss due to forward flight. Forward flight conditions caused separation

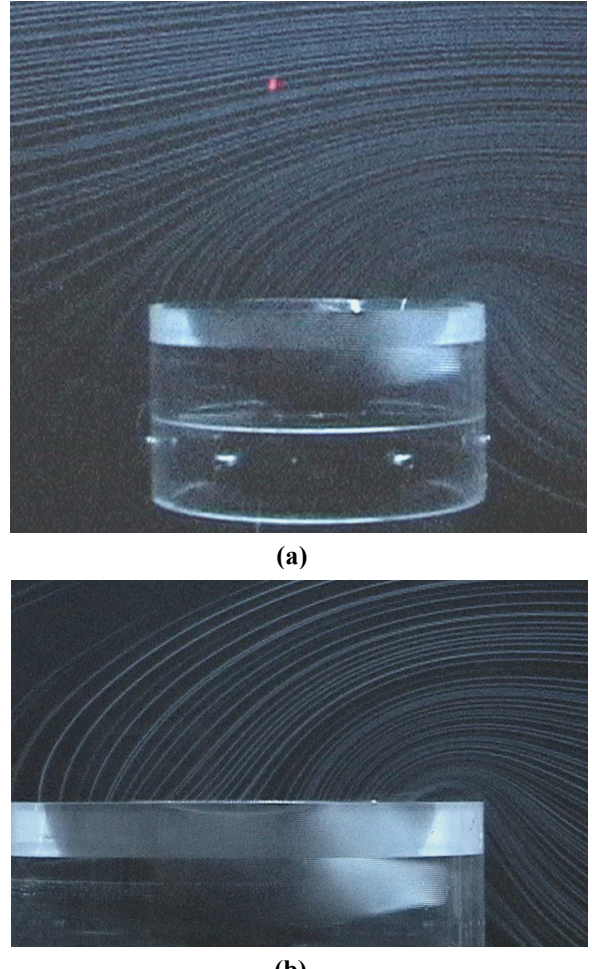


Figure 10. Smoke visualization at 6000 rpm and 5 m/s.

from the rotor hub in this highly three dimensional and complex inlet flow environment. The existence of inlet lip separation arranged the streamlines at the inlet section in such a way that a more pronounced impingement of the inlet flow on the hub surface was observed. The hub separation occurring only near the 0° location was a direct result of the lip separation.

At 90° and 270° circumferential locations, the forward flight velocity affected the radial total pressure distribution and resulted in an increase in the losses near the tip region. There was more total pressure defect at 90° circumferential location. Since the measurements were performed at the downstream of the fan rotor, the effect of rotational direction of the fan rotor was noticed at 90° circumferential location. Because of counter-clockwise direction of the fan rotor, the re-circulatory low momentum fluid originating from the leading side (0° location) was effectively transported to 90° location. The defect in total pressure was more enhanced because of counter-clockwise direction of the fan rotor. In forward flight, the relative inlet velocity vector at the inlet plane changes its magnitude at each circumferential position. This was one of the reasons for the axisymmetric non-uniformity of the rotor exit total pressure field.

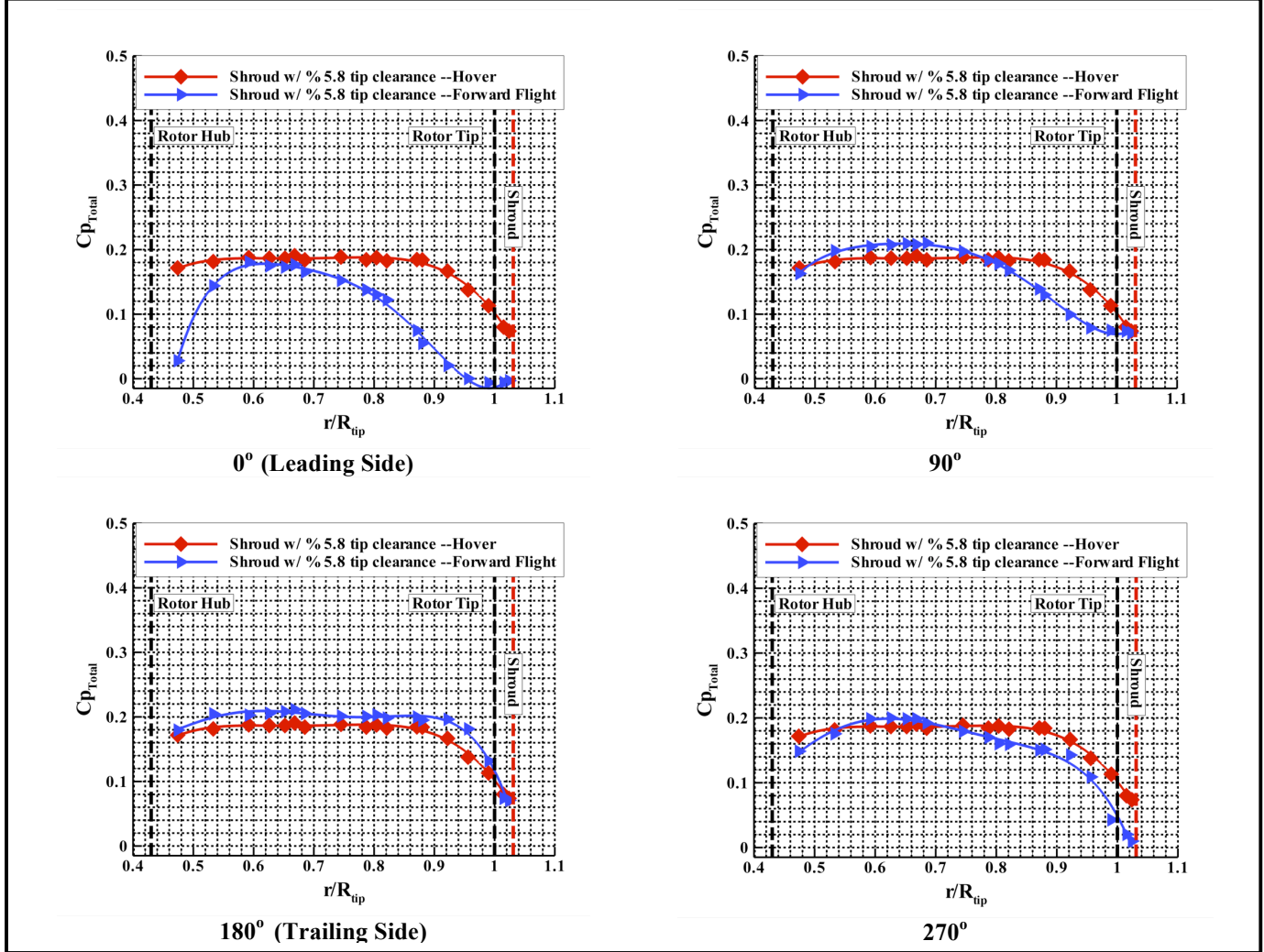


Figure 11. Comparison of hover and forward flight at 12000 rpm and 10 m/s forward flight speed.

Unlike the leading side, the trailing side of the ducted fan was positively affected from forward flight velocity. The measured rotor exit total pressure in forward flight mode at all spanwise locations was slightly higher than that of hover. The significant inlet lip separation related momentum defect did not exist in the trailing side. The total pressure in front of the rotor at the trailing side was slightly higher than that of hover condition altering the blade loading near the tip section. It was obvious from Figure 11 that the tip related losses were slightly reduced in forward flight. Because of higher momentum fluid impinging on the inner casing near the trailing side, the adverse effect of tip leakage flow was slightly reduced. The rotor tip was performing better compared to hover condition. The flow impingement on the inner casing near the trailing side was a potential drag source in the forward flight zone.

Effect of Tip Clearance in Forward Flight

Effect of tip clearance at forward flight condition at 12000 rpm and 10 m/s forward flight speed is shown in

figure 12. Like the hover condition, decreasing the tip gap height increased total pressure distribution in forward flight. When tip gap height was reduced, the tip leakage flow rate was also reduced resulting in smaller tip vortex. The interaction of the smaller leakage vortex and inlet lip separation was controlled more effectively. For other circumferential stations, behavior of total pressure distribution with a change in tip clearance resembled to the ones that were obtained for hover condition.

Forward Flight Penalty

Transition to forward flight resulted in an increase in losses at the inlet lip region. It also enhanced tip region generated losses of the fan rotor. For a better understanding and comparison of forward flight and hover condition related flow physics, a forward flight penalty (FFP) was defined.

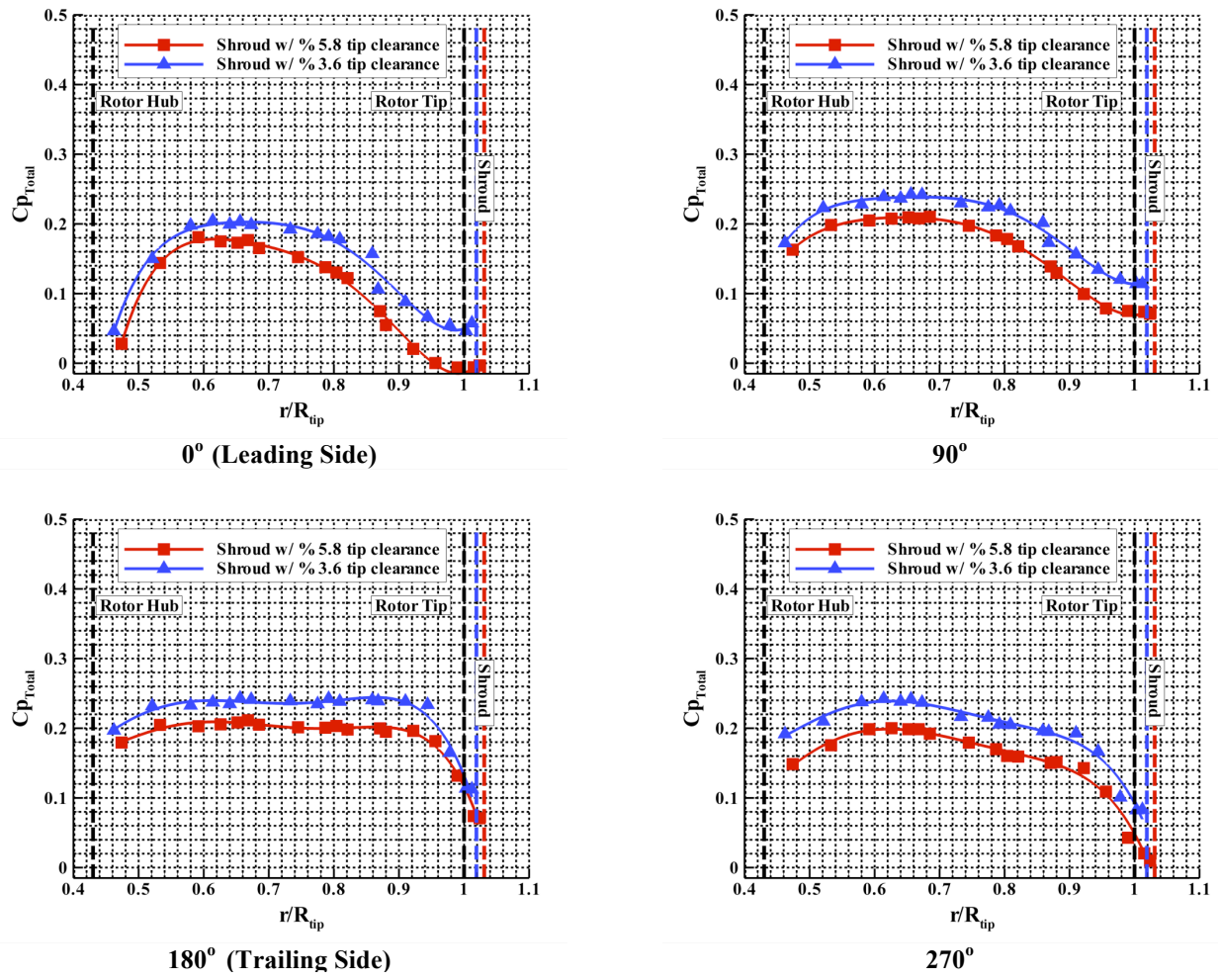


Figure 12. Comparison of tip clearance effect at forward flight at 12000 rpm and 10 m/s forward flight speed.

FFP was an indicator of total pressure loss generated for a configuration at forward flight in comparison to hover condition.

$$FFP = \frac{Cp_{T\{H\}} - Cp_{T\{FF\}}}{Cp_{T\{H\}}} \quad (3)$$

Figure 13 shows FFP calculated for the measurements performed at 10 m/s forward flight velocity for 12000 rpm rotor speed for both tip clearances. Since the most significant loss generation due to forward flight occurred at the leading side, FFP was calculated at that location. FFP values closer to zero indicates minimum loss generated regions due to forward flight. This is only locally possible at the mid-span of the rotor where forward flight related flow problems are minimal. FFP=1 may result in when the rotor exit total pressure is at atmospheric level corresponding to a local stagnation zone which may occur in low momentum separated flow areas.

Both tip configurations experienced a total pressure loss in forward flight. As discussed earlier, inlet flow distortion was the main reason for the loss generation in forward flight.

Although the shroud with smaller tip clearance experienced some total pressure loss, the shroud with larger tip clearance increased the total pressure loss tremendously. Especially near the tip region, increasing the tip gap height doubled the total pressure loss. The larger tip clearance resulted in a larger tip leakage vortex. Because the tip vortex size was increased, the effect of inlet lip separation was enhanced and fan rotor performance dropped dramatically. The effect of tip leakage and inlet lip separation was not only influencing the tip region.

It was also observed that both shrouds generated a significant amount of loss near the hub region. However loss generated near the hub was not dependent on tip clearance magnitude in forward flight.

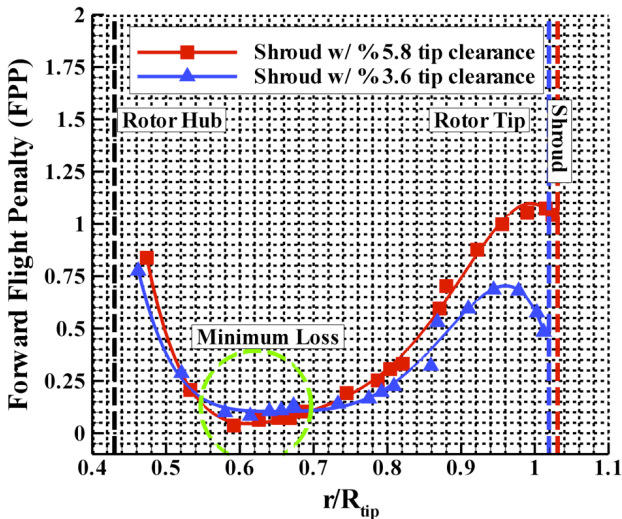


Figure 13. Forward flight penalty calculated at 12000 rpm and 10 m/s forward flight speed.

Effect of Forward Flight Speed

The total pressure measurements at the leading side were also conducted for different forward flight speeds at 12000 rpm. Figures 14 and 15 show measurement results for %5.8 and %3.6 tip clearances respectively. The total pressure loss was increased by forward flight velocity. For lower speeds, the regions near the rotor tip was affected. As the flight speed was increased, inlet flow distortion related effects were pronounced as shown in figure 14. For 20 m/s it was obvious that the rotor had tremendous difficulty to breath and unsteady effects were dominant.

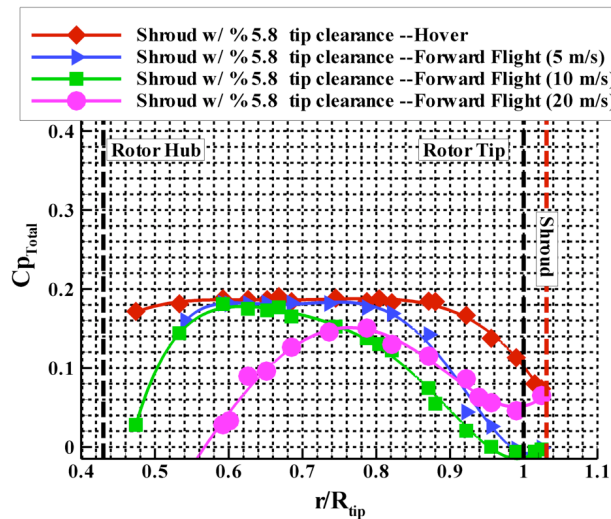


Figure 14. Effect of forward flight speed for %5.8 tip clearance.

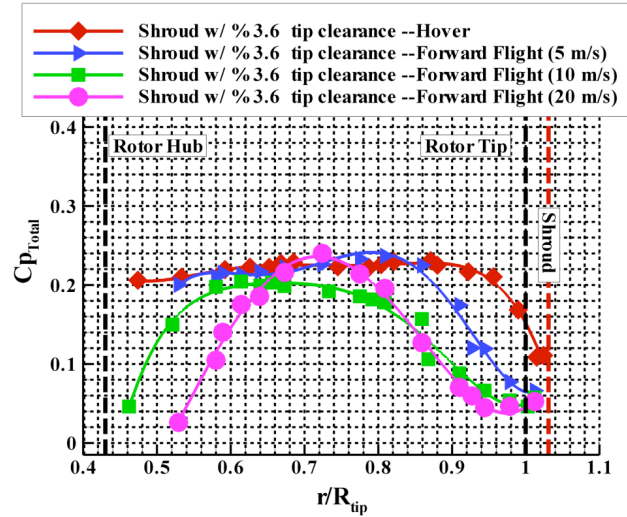


Figure 15. Effect of forward flight speed for %3.6 tip clearance.

Figure 15 shows the total pressure losses at %3.6 tip clearance for hover and all other forward flight conditions. The qualitative shape of the loss curves in spanwise direction were very similar to that of 5.8% clearance. There was a visible reduction in overall total pressure distributions as shown in Figure 15. Although the mid span of the blade had acceptable total pressure values, the hub and tip region total pressures were somewhat lower than that of hover results.

Computational Results

Three dimensional computational methods can be used for analyzing viscous and turbulent flow field around and inside the ducted fan for hover and forward flight conditions. High resolution total pressure results experimentally obtained in this study constitute a good set of data for validation of computational algorithms. Although we do not present a complete set of computational results in this paper, a brief assessment of our computational approach against the measured data is provided.

Figure 16 shows computed streamlines around the fan rotor blade at 12000 rpm. The numerical solution for the ducted fan used in this study is obtained by using a commercial fluid flow solver developed by ANSYS. A fully turbulent computation of the Reynolds Averaged Navier-Stokes equations using a coupled finite volume formulation with 7.5 million cells provides a prediction of the flow around and inside the current ducted fan system. A detailed computational investigation of this ducted fan model is in progress.

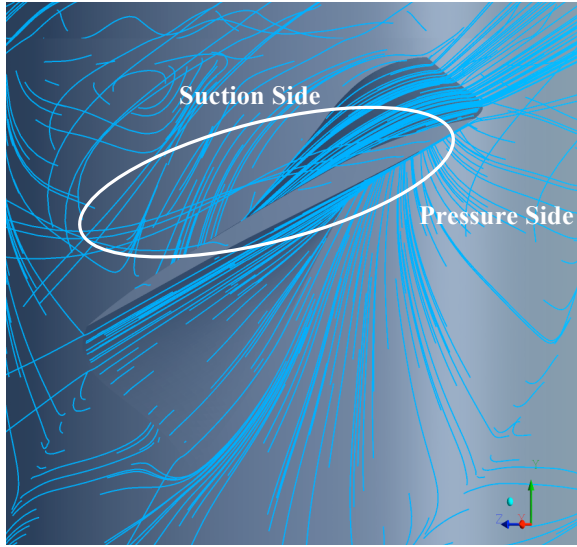


Figure 16. Streamlines drawn at rotor tip region with computational results at hover condition at 12000 rpm .

The computational results are obtained at 12000 rpm for hover condition. Figure 17 shows comparison of experimental and computational results. In this unsteady rotor computation, Circumferentially averaged total pressure values computed at the exit of the fan rotor is compared to the experimental results. The computational and experimental results show very good agreement in the spanwise distribution except in a limited area near the hub where $r/R_{Tip} < 0.6$. The computational results somewhat deviate from experimental results near the hub region. That is because of the highly complex low Reynolds number turbulent flow field near the hub region. A combination of high rotational speed and low Reynolds number characteristic of the flow makes this computation highly challenging.

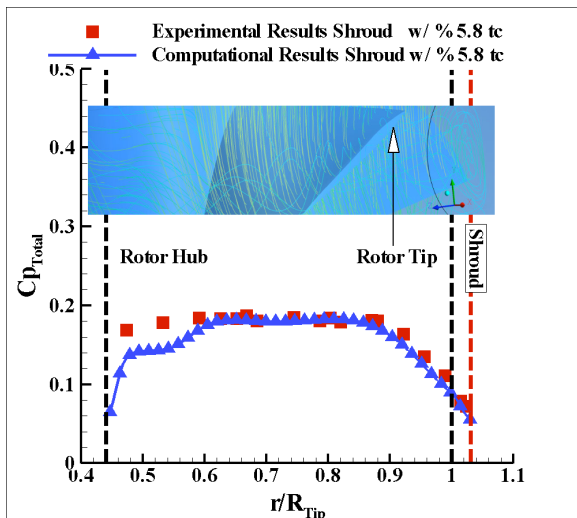


Figure 17. Comparison of experimental results to computational results at hover condition at 12000 rpm .

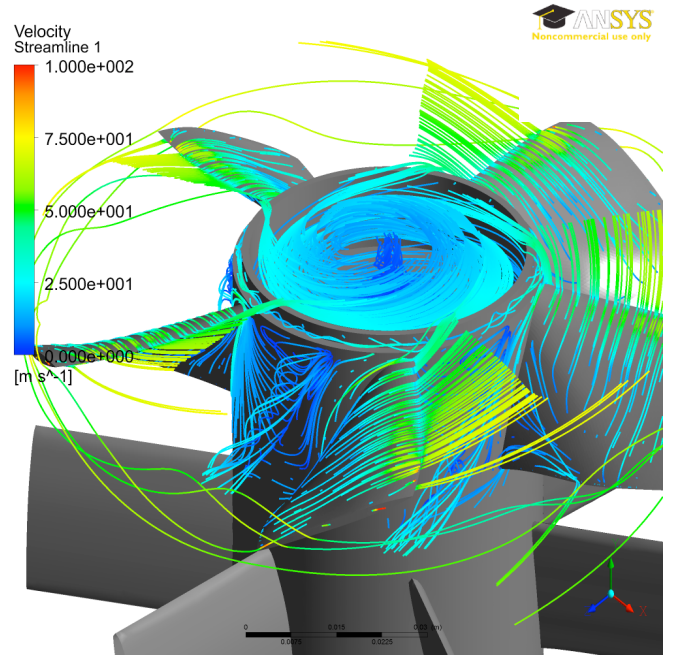


Figure 18. Computationally obtained streamlines near the ducted fan at 12000 rpm, in the relative frame of reference.

CONCLUSIONS

In this study, an experimental investigation around a ducted fan for VTOL UAV applications was carried out. Total pressure measurements at the exit of the fan rotor to investigate the effect of tip leakage flow in hover and forward flight conditions were obtained in a low speed low turbulence wind tunnel.

Ducted fans offer higher disk loading compared to open rotors. Using a ducted fan improved hover disk loading up to %24 compared to the open rotor.

Tip clearance is one of the most important parameters affecting ducted fan rotor performance. Decreasing tip clearance from %5.8 to %3.6 increased fan rotor exit total pressure by %17 at mid span for hover condition. Hover tests also indicated that smaller tip gap increased overall performance of fan rotor along the span wise direction.

Exit total pressure of the fan rotor was measured at 4 circumferential stations during forward flight.

The most significant total pressure losses occurred at the leading side (0°) for forward flight condition. Distortions at the inlet of the fan rotor and inlet lip separation stalled the tip of the rotor blade and resulted in a performance loss along %80 of blade span.

Unlike leading side, the trailing side of the ducted fan is positively affected from forward flight velocity. More favorable inlet flow conditions near the trailing side of the rotor leads to a more effective rotor energy addition process.

Decreasing tip gap height enhanced total pressure distribution in forward flight mode. The total pressure loss near the tip of the blade is decreased by reducing the tip gap height.

Especially near the tip region increasing tip gap height by approximately %40, doubled the total pressure loss at the leading side of the ducted fan at forward flight. The effect of tip leakage and inlet lip separation was spread overall blade span.

Forward flight conditions caused separation from the rotor hub in this highly three dimensional and complex inlet flow environment. The existence of inlet lip separation arranged the streamlines at the inlet section in such a way that a more pronounced impingement of the inlet flow on the hub surface was observed.

The total pressure loss was increased by forward flight velocity. For lower speeds, the regions near the rotor tip was affected. As the flight speed was increased, inlet flow distortion related effects were pronounced. For 20 m/s it was obvious that the rotor had tremendous difficulty to breath and unsteady effects were dominant.

The preliminary results from a 3D computational results using Reynolds Averaged Navier Stokes equations showed very good agreement with the measured total pressure distributions at the rotor exit. The current experimental results form a high resolution data set for computational validation efforts that are essential for ducted fan development studies.

Total pressure data sets obtained at various flight speeds and tip clearance values are also useful in generating design correlations.

ACKNOWLEDGMENTS

The authors acknowledge the financial support provided by the PSU Vertical Lift Center of Excellence VLRCOE. They wish to thank to Dr. Jeremy Veltin for his help in flow visualization part of the current experiments. They are also indebted to Mr. Rick Auhl for his help with the wind tunnel operation and Mr. Harry Houtz for his technical support.

REFERENCES

1. Abrego, A. I. and Bulaga, R. W., 2002, "Performance Study of a Ducted Fan System," AHS Aerodynamics, Aeroacoustic, Test and Evaluation Technical Specialist Meeting.
2. Martin, P. and Tung, C., 2004, "Performance and Flowfield Measurements on a 10-inch Ducted Rotor VTOL UAV," AHS 60th Annual Forum of American Helicopter Society, Baltimore, MD.
3. Fleming, J., Jones, T., Lusardi, J., Gelhausen, P., and Enns, D., 2004, "Improved Control of Ducted Fan VTOL UAVs in Crosswind Turbulence," AHS 4th Decennial Specialist's Conference on Aeromechanics.
4. Graf, W., Fleming, J., and Wing, Ng., 2008, "Improving Ducted Fan UAV Aerodynamics in Forward Flight," 46th AIAA Aerospace Sciences Meeting and Exhibit , Reno, Nevada.
5. Akturk, A., Shavalikul, A., and Camci, C., 2009, "PIV Measurements and Computational Study of a 5-Inch Ducted Fan for V/STOL UAV Applications," 47th AIAA Aerospace Sciences Meeting and Exhibit , Orlando, Florida.
6. Mort, K.W. and Yaggy, P.F., 1962, "Aerodynamic Characteristics of a 4-Foot-Diameter Ducted Fan Mounted on the Tip of a Semispan Wing," NASA TND-1301.
7. Yaggy, P.F. and Mort, K.W., 1961, "A Wind-TunnelInvestigation of a 4-Foot-Diameter Ducted Fan Mounted on the Tip of a Semispan Wing," NASA TND-776.
8. Mort, K.W. and Gamse, B., 1967, "A Wind Tunnel Investigation of a 7-Foot-Diameter Ducted Propeller," NASA TN D-4142.
9. United Sensors Corporation Kiel probe: general information. Retrieved April 01, 2010, from <http://www.unitedsensorcorp.com/kiel.html>.